International Journal of Heat and Technology
Vol. 42, No. 6, December, 2024, pp. 1911-1923
Journal homepage: http://iieta.org/journals/ijht

Development of an Anomaly Detection Model for Bridge Vibration Acceleration under Temperature Variations and Investigation of Thermodynamic Mechanisms

Jiting Zhan*, Kui Hu, Chao Xue

China Electric Construction Road and Bridge Group Corporation., Urumqi 830000, China

Corresponding Author Email: lqzhanjt@powerchina.cn

https://doi.org/10.18280/ijht.420608

Received: 7 July 2024
Revised: 23 November 2024
Accepted: 2 December 2024
Available online: 31 December 2024

Keywords:
bridge health monitoring, vibration acceleration, anomaly detection, temperature variations, machine learning

ABSTRACT

Bridges play a critical role in transportation systems, making their long-term operational safety an urgent concern. The vibration characteristics of bridges are influenced by various external factors, including temperature, load, and wind. Among these, temperature fluctuations significantly affect the dynamic response of bridge structures. Thermal expansion and contraction of bridge materials induced by temperature changes can alter vibration characteristics, impacting the accuracy of structural health monitoring. Traditional bridge health monitoring methods primarily rely on static analysis and manual inspections. However, under complex environmental conditions, particularly with significant temperature variations, these methods struggle to provide accurate and real-time monitoring results. Recently, vibration acceleration-based anomaly detection methods have garnered research attention, yet the influence of temperature on vibration characteristics remains insufficiently addressed. Current studies predominantly focus on applying machine learning and deep learning techniques to bridge vibration anomaly detection but often neglect the disruptive effects of temperature variations, limiting their adaptability and accuracy in real-world applications. To address this issue, this study analyzes bridge vibration characteristics under varying temperature conditions, constructs a temperature-inclusive vibration acceleration dataset, and proposes a novel anomaly detection model to enhance detection precision and robustness. The findings offer a new perspective for bridge health monitoring and provide theoretical insights for managing and maintaining bridges under temperature variations.

1. INTRODUCTION

With the rapid development of modern transportation, the safety and stability of bridges, as critical transportation infrastructure, have garnered increasing attention. Bridges are subjected to long-term influences from external factors such as temperature, wind, and traffic loads, resulting in changes in their structural vibration characteristics, and in some cases, damage or fatigue. Particularly in regions with significant temperature variations, temperature fluctuations can cause thermal expansion or contraction of bridge materials, thereby altering the vibration modes and dynamic characteristics of the structure [1-5]. Therefore, effectively monitoring and analyzing the vibration characteristics of bridges under temperature variations has become an important issue for ensuring the safe operation of bridges [6-11].

To address the issue of bridge safety monitoring, traditional health monitoring methods primarily rely on analyzing the static characteristics of the structure or conducting periodic manual inspections. However, these methods have certain limitations, especially when dealing with dynamic characteristic changes induced by environmental variations, making it challenging to obtain real-time and accurate information about the bridge's condition. With advancements in sensor technology, data acquisition techniques, and big data analysis methods, vibration signal-based bridge health monitoring approaches have become a research hotspot. Particularly under complex conditions such as temperature variations, performing anomaly detection using vibration acceleration data enables the precise capture of subtle changes in the bridge's condition, providing scientific support for early fault warnings and maintenance decisions [12-17].

Existing methods for anomaly detection in bridge vibration acceleration primarily rely on statistical analysis, machine learning, or deep learning models. Although these methods have achieved certain results under standard testing conditions, in practical applications, the influence of temperature variations on bridge vibration characteristics is often insufficiently considered [18-20]. Many existing methods overlook the interference effects of temperature variations on vibration acceleration signals, and most models fail to effectively address the complexity and variability of bridge vibration characteristics [21-24]. Consequently, the applicability and accuracy of current research methods under temperature variation conditions remain limited, necessitating further innovation and optimization.

This paper aims to address the shortcomings of existing research by focusing on anomaly detection of bridge vibration acceleration under temperature variations. Firstly, the specific impact mechanism of temperature on vibration characteristics

is explored through an analysis of bridge vibration characteristics under temperature variations. Secondly, a bridge vibration acceleration dataset incorporating temperature variation factors is constructed, and features are extracted and analyzed in conjunction with temperature data. Finally, a bridge vibration acceleration anomaly detection model adaptable to temperature variations is proposed, aiming to improve detection accuracy and robustness. This study not only provides a novel detection method for bridge health monitoring but also offers theoretical support and practical guidance for bridge maintenance and management under temperature variation conditions.

2. ANALYSIS OF BRIDGE VIBRATION CHARACTERISTICS UNDER TEMPERATURE VARIATIONS

Under temperature variation conditions, the vibration characteristics of bridges often exhibit complex changes. Temperature rise and fall directly affect the geometry and material properties of bridge components, particularly for metal and concrete structures. Temperature variations lead to material expansion or contraction, thereby altering the structural stiffness and centroid position of the bridge. These changes can cause variations in vibration frequencies and even changes in vibration modes. Specifically, when a bridge experiences temperature fluctuations, the elastic modulus of materials such as reinforcement bars or prestressed steel cables exhibits temperature-dependent changes, resulting in stiffness fluctuations that affect the amplitude and frequency of the vibration response. Moreover, temperature variations are often closely related to the motion state of the bridge, influencing the vibration acceleration signals and forming a unique temperature-vibration response relationship. Without proper analysis and identification, these responses can easily be confused with actual fault signals. Therefore, analyzing the impact of temperature variations on bridge vibration characteristics not only helps reveal the structural response characteristics caused by temperature changes but also provides theoretical support for subsequent vibration acceleration data analysis and anomaly detection.

In the process of constructing an anomaly detection model for bridge vibration acceleration, it is essential to investigate the thermodynamic mechanisms under temperature variations. Temperature changes are not only a physical phenomenon but also induce changes in the thermal stress distribution and strain states within the bridge materials. These thermal stress changes can cause localized deformation, crack propagation, or looseness at connection points, leading to anomalies in vibration characteristics. Such anomalies may manifest as sudden changes, amplitude variations, or frequency shifts in vibration acceleration signals. If these structural response characteristics caused by temperature changes are not taken into account, normal temperature fluctuations might be misidentified as fault signals, thereby affecting the accuracy and reliability of anomaly detection.

2.1 Finite element analysis of bridge vibration

In finite element analysis, the vibration behavior of a bridge is typically described by its dynamic equations. The influence of temperature variations on bridge structures is reflected in changes in the physical properties of materials, such as elastic modulus and expansion coefficients, which further affect the stiffness and mass distribution of the structure. Therefore, when establishing finite element dynamic equations under temperature variation conditions, these temperature-induced changes must be considered. The finite element model constructed in this study divides the bridge structure into a finite number of elements, decomposing the overall dynamic behavior into the local behavior of each element. The vibration response of each element is described by the mass matrix and stiffness matrix, both of which are adjusted based on temperature variations. Temperature changes affect not only material stiffness but also the mass distribution of the structure, and these combined effects determine the vibration characteristics of the bridge. Assuming the mass matrix is represented by L, the damping matrix by Z, the elastic stiffness matrix by J, and the external load vector by d, the finite element dynamic equation is expressed as follows:

$$L\ddot{\delta} + Z\dot{\delta} + J\delta = d \tag{1}$$

In the analysis of free vibration in bridges, it is typically assumed that the structure is undamped, resulting in the undamped free vibration equation. The purpose of the undamped free vibration equation is to describe the free vibration process of a bridge excited by initial conditions without external forces. Under temperature variation conditions, the physical properties of materials (e.g., elastic modulus) change with temperature, leading to the degradation of bridge stiffness. This implies that the stiffness matrix of the bridge adjusts with temperature fluctuations, thereby affecting its vibration frequencies and modes. Consequently, in analyzing free vibration under the influence of temperature, it is necessary to model the stiffness changes induced by temperature variations and incorporate them into the undamped free vibration equation. Assuming the overall mass matrix is represented by L, composed of the element mass matrices L^r, the undamped free vibration equation is given as:

$$L\ddot{\delta} + J\delta = 0 \tag{2}$$

By solving the eigenvalue problem of the dynamic equation, the natural frequencies and corresponding vibration modes of the bridge can be obtained. Under temperature variation conditions, changes in the stiffness matrix and mass matrix result in variations in the bridge's natural frequencies. Solving the eigenvalue problem essentially involves finding a set of frequencies and modes that satisfy the dynamic behavior of the structure under temperature variation conditions. The solution to the eigenvalue problem can be obtained by solving a specific mathematical equation, yielding the natural frequencies and modes of the bridge under particular temperature conditions. These frequencies and modes reflect the inherent response characteristics of the bridge under temperature variations and provide critical references for further vibration acceleration analysis, health monitoring, and anomaly detection. The expression for the element mass matrix is as follows:

$$L^r = \iiint V^S \vartheta V f N \tag{3}$$

In finite element analysis, the mass matrix of a bridge is a key matrix used to describe the mass distribution within the structure. The mass matrix of the bridge is not only related to

the geometry and material density of the structure but also closely related to temperature variations. Temperature changes affect the density of materials, thereby influencing the computation of the mass matrix. Specifically, when the temperature rises or falls, the density of bridge components may change, necessitating the incorporation of temperature dependency into the calculation of the mass matrix. For instance, by integrating the mass matrix of each element, the mass distribution of each element can be obtained, which varies under temperature fluctuations. The element mass matrix of the beam obtained through integration is as follows:

$$L^{r} \approx \vartheta X \int_{0}^{V} V^{S} V da = \frac{\vartheta X \Delta M}{418} \begin{bmatrix} 154 & 21\Delta M & 56 & -14\Delta M \\ 21\Delta M & 4\Delta M^{2} & 14\Delta M & -3\Delta M^{2} \\ 54 & 14\Delta M & 156 & -21\Delta M \\ -14\Delta M & -3\Delta M^{2} & -21\Delta M & 4\Delta M^{2} \end{bmatrix} \tag{4}$$

Assuming that the frequency of free vibration of the structure is represented by μ, the solution of Eq. (2) can be expressed as:

$$\delta(s) = \psi SIN \mu s \tag{5}$$

By combining the above equation with Eq. (2), the following is obtained:

$$\left(J - \mu^{2} L\right)\psi = 0 \tag{6}$$

The natural frequency of a bridge under temperature variation conditions is an important parameter for describing its free vibration characteristics. The free vibration frequency of the structure is directly influenced by its mass matrix and stiffness matrix, both of which vary with temperature changes. Therefore, in the finite element analysis process, solving the natural frequency of the structure under temperature variation conditions requires fully considering the changes in mass and stiffness induced by temperature. During the solution process, adjustments to the mass matrix and stiffness matrix under temperature variations allow the natural frequency μ of the bridge under different temperature conditions to be obtained. The variation in frequency directly reflects how the vibration characteristics of the bridge change with temperature, providing a foundation for health monitoring, vibration anomaly detection, and subsequent structural assessment of the bridge.

2.2 Thermal vibration analysis of bridges

Under temperature variation conditions, the vibration characteristics of bridges are influenced not only by material stiffness and mass but also by changes in external loads, such as axial and transverse forces. Temperature changes induce thermal expansion in various parts of the bridge, thereby affecting the internal force state of the structure. For instance, as the temperature increases, the bridge components expand, generating axial and transverse forces, which alter the overall stiffness distribution of the bridge and, subsequently, its vibration characteristics. In finite element analysis, the internal force variations caused by temperature changes need to be precisely modeled to ensure that the dynamic equations accurately reflect the stress state of the bridge under different temperature conditions. The axial and transverse forces under temperature variation conditions are typically described by introducing a temperature field and incorporating the thermal expansion coefficient and material properties to depict the deformation and stress states of individual components. These changes can cause shifts in the vibration frequencies of the bridge and may also lead to changes in the vibration modes. This is particularly significant under conditions of large temperature gradients, where local deformations and force variations may trigger uneven vibration responses. Assuming the structural bending stiffness matrix is represented by J_m, the geometric stiffness matrix by J_H, the total stiffness matrix by J_m+J_H, and the mass matrix by L, the thermal vibration equation of the bridge structure under temperature variation conditions can be established as follows:

$$\left(J_m + J_H - \mu^{2} L\right)\psi = 0 \tag{7}$$

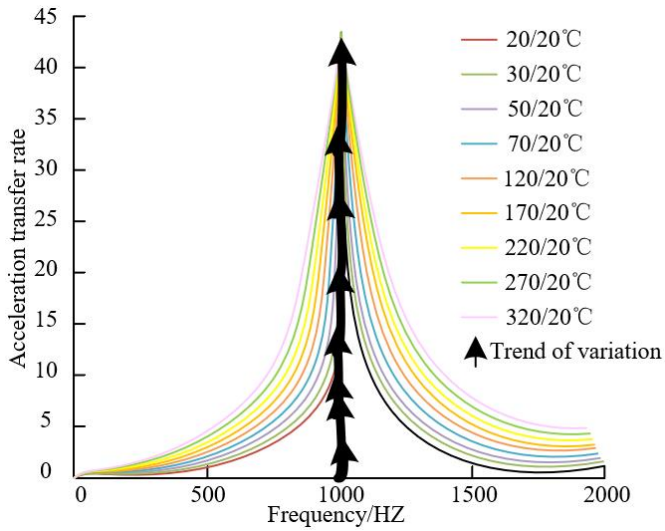

Figure 1. Trend of bridge vibration acceleration with vibration frequency under different temperature differences

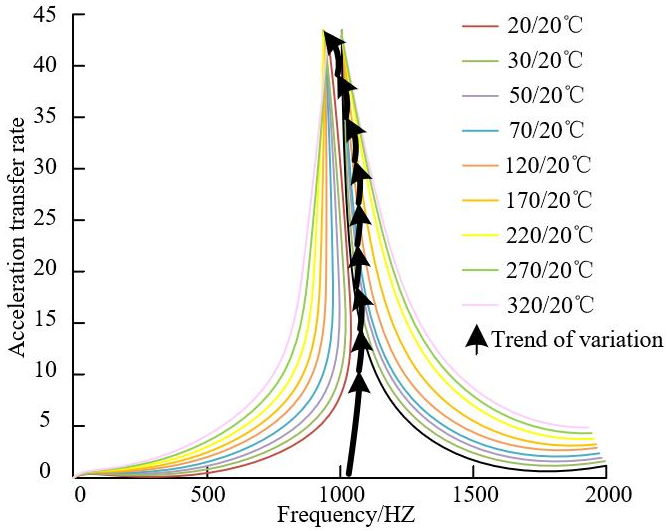

Figure 2. Trend of bridge vibration acceleration with vibration frequency considering both temperature differences and thermal elastic modulus

Bridge vibration acceleration is an important indicator of vibration intensity and is closely related to the vibration characteristics of the bridge. Under temperature variation conditions, changes in the vibration characteristics of the bridge lead to corresponding changes in vibration acceleration. If the natural vibration frequency of the bridge decreases, the vibration acceleration will increase under the same external excitation because the flexibility of the structure increases, resulting in greater displacement and higher acceleration. Conversely, if the temperature decreases, leading to an increase in the stiffness of the bridge and a rise in its natural vibration frequency, the vibration acceleration will decrease under the same excitation. Figures 1 and 2 illustrate the trends of bridge vibration acceleration with vibration frequency under different temperature differences and considering both temperature differences and thermal elastic modulus, respectively.

3. CONSTRUCTION OF VIBRATION DATASET OF BRIDGES UNDER TEMPERATURE VARIATIONS

This study takes the wind-induced vibration response monitoring system of the Toutunhe Interchange Main Bridge in Urumqi, Xinjiang, as the research object to carry out research on anomaly detection algorithms for acceleration data measured during the bridge construction phase. The bridge is located in a low-mountain valley topography, with a total length of 2292 m, a deck width of 19 m, and a height of 123.8 m. The main structure is oriented east-west. The main bridge is a continuous rigid-frame cast-in-place box girder with spans of 82+4×150+82 m. The substructure adopts pile foundations, and the piers are variable-section hollow piers, with a maximum pier height of 114.8 m. Piers 3 and 4, located in the valley terrain and subject to strong wind effects, were selected as the primary measurement objects. The construction site is shown in Figure 3.

Figure 3. Construction site

When constructing the vibration acceleration dataset of the bridge, it is necessary to comprehensively consider the impact of temperature variations on the vibration characteristics of the bridge and arrange the sensors accordingly. First, the vibration characteristics of the bridge undergo significant changes with temperature variations, particularly due to axial and transverse force changes, which may result in shifts in vibration modes. Therefore, during the construction of the dataset, vibration acceleration sensors need to be installed at several key locations on the bridge. Specifically, two JM3873G accelerometers were installed on each side of the cantilever at one-quarter span from the piers during cantilever construction. Data were transmitted remotely via wireless communication. Each accelerometer was equipped with two high-precision low-frequency vibration pickups, which collected four-directional acceleration (longitudinal, transverse, vertical, and torsional) at one-quarter span positions on the cantilever. The sampling frequency was set to 64 Hz. The specific instrumentation layout is shown in Figure 4.

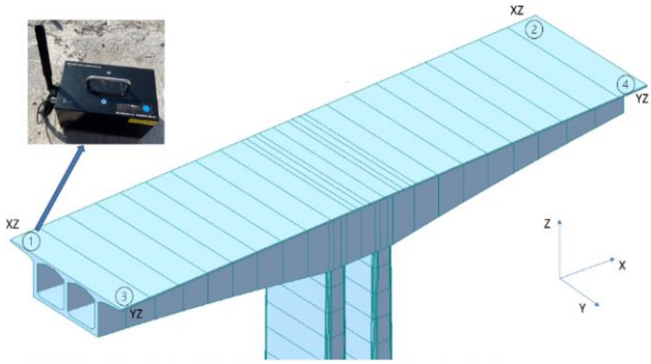

Figure 4. Schematic diagram of instrument placement (①, ②, ③, and ④ are biaxial accelerometers)

Under temperature variation conditions, in addition to acceleration sensors, this study also deployed temperature sensors and strain gauges to synchronously record temperature changes and structural stress states. Temperature sensors were placed on the bridge surface and at key structural locations to accurately monitor environmental temperature and the bridge's own temperature changes. Strain gauges were used to capture changes in internal forces of the bridge caused by temperature variations, especially axial and lateral forces. By combining data from temperature sensors and strain gauges, a more comprehensive understanding of the impact of temperature changes on the vibration characteristics of the bridge can be achieved.

4. VIBRATION ACCELERATION ANOMALY DETECTION MODEL FOR BRIDGES UNDER TEMPERATURE VARIATION CONDITIONS

4.1 Anomaly Transformer model

The Anomaly Transformer model achieves this by alternately stacking Anomaly-Attention blocks and feedforward layers. This stacking structure facilitates learning underlying correlations from deep multi-level features. The Anomaly Transformer model is shown in Figure 5.

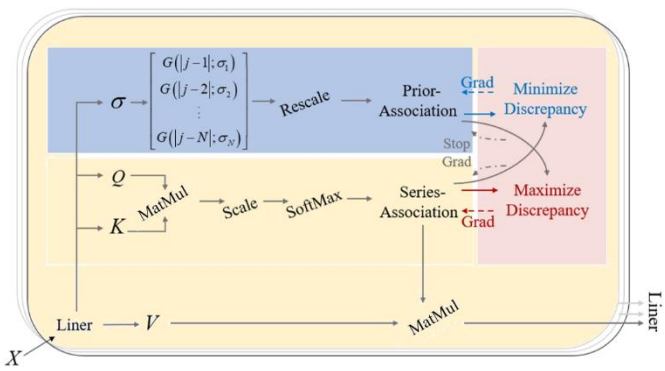

Figure 5. Anomaly Transformer model

Assume the model has L layers. For an input time series X of length N, the formula for the l-th layer is formalized as:

$$\begin{aligned} Z^{l} &= Layer-Norm(Anomaly-Attention(X^{l-1})+X^{l-1}) \\ X^{l} &= Layer-Norm(Feed-Forward(Z^{l})+Z^{l}) \end{aligned} \tag{8}$$

where, X^l represents the output of the l-th layer with d_{model} channels. X^0=*Embedding*(X) represents the embedded raw sequence. Z^l denotes the hidden state of the l-th layer. *Anomaly-Attention*( ) calculates the association difference.

4.1.1 Anomaly-Attention

The Anomaly-Attention mechanism adopts a dual-branch structure, addressing the limitation of the single-branch self-attention mechanism in traditional Transformers, which fails to model both prior and sequence associations simultaneously. The Anomaly-Attention mechanism captures both global and local associations within the input sequence. For the prior association branch, a learnable Gaussian kernel function is introduced to construct local associations for each time point, ensuring that anomalous points are more likely to establish strong associations with their neighboring time points, thereby better capturing local anomalies. By employing a learnable scale parameter σ, prior associations can adapt to various time-series patterns. The sequence association branch learns the global dynamics of the entire bridge acceleration sequence through a self-attention mechanism, aiding in identifying anomalous vibration patterns. The Anomaly-Attention mechanism in the l-th layer is represented by the following equations:

$$\begin{aligned} &Initialization: \\ &Q,K,V,\sigma = X^{l-1}W_Q^l, X^{l-1}W_K^l, X^{l-1}W_V^l, X^{l-1}W_\sigma^l \end{aligned} \tag{9}$$

where, Q, K, V, σ represent the query, key, value, and learnable scale of the self-attention layer. W_Q^l, W_K^l, W_V^l, W_σ^l denote the parameter matrices of Q, K, V, σ in the l-th layer.

$$\begin{aligned} &Prior\text{-}Association: \\ &P^{l} = Rescale\left(\left[\frac{1}{\sqrt{2\pi}\sigma_i} exp(-\frac{|j-i|^2}{2\sigma_i^2})\right]_{i,j\in\{1,,N\}}\right) \end{aligned} \tag{10}$$

The prior association is generated based on the learned scale σ. The association weight between the i-th and j-th time points is calculated using the Gaussian kernel as follows:

$$G(|j-i|;\sigma_i) = \frac{1}{\sqrt{2\pi}\sigma_i} exp\left(-\frac{|j-i|^2}{2\sigma_i^2}\right) \tag{11}$$

In addition, *Rescale*( ) is used to transform the association weight into a discrete distribution P^l:

$$Series\text{-}Association: S^{l} = Softmax\left(\frac{QK^T}{\sqrt{d_{model}}}\right) \tag{12}$$

where, S^l represents the sequence association, where *softmax*( ) normalizes the attention map along the last dimension:

$$Reconstruction: \hat{Z}^{l} = S^{l}V \tag{13}$$

$\hat{Z}^l$ represents the hidden representation after the Anomaly-Attention mechanism in the l-th layer:

4.1.2 Association difference

Due to the rarity of anomalous points and the dominance of normal patterns, anomalous points are less likely to establish strong associations with the entire sequence, and their associations are more likely concentrated on adjacent time points. Thus, the association difference for anomalous points is typically smaller than that of normal points. The association difference is formalized as the symmetric KL divergence between the prior association and the sequence association, representing the information gain between these two distributions. The association difference for multi-layer associations is averaged to combine associations from multi-level features into a more informative metric:

$$\begin{aligned} &\text{AssDis}(P,S;X) \\ &= \left[\frac{1}{L}\sum_{l=1}^{L}\left(\text{KL}(P_{i,:}^{l}\|S_{i,:}^{l})+\text{KL}(S_{i,:}^{l}\|P_{i,:}^{l})\right)\right]_{i=1,\cdots,N} \end{aligned} \tag{14}$$

where, *KL*( ) calculates the KL divergence between two discrete distributions P^l and S^l for each row. *AssDis*(P,S;X) represents the pointwise association difference for X relative to multi-layer prior associations P and sequence associations S.

4.1.3 Anomaly criteria based on association difference

We incorporate normalized association differences into the reconstruction criteria, and the final anomaly score X is expressed as:

$$\begin{aligned} &\text{AnomalyScore}(X) \\ &= \text{Softmax}\left(-\text{AssDis}(P,S;X)\right)\odot[\|X_{i,:}-X_{i,:}\|_2^2]_{i=1,\cdots,N} \end{aligned} \tag{15}$$

where, $\odot$ denotes element-wise multiplication. *AnomalyScore*(X) represents the pointwise anomaly criteria of X. To improve reconstruction, anomalies typically reduce the association difference, which still results in higher anomaly scores. Thus, this design enables the reconstruction error and the association difference to jointly enhance anomaly detection performance.

4.2 Bi-LSTM-based anomaly data reconstruction algorithm

Due to factors such as monitoring sensor failures, network interruptions, or on-site disturbances, the monitored data inevitably contains outliers. To reconstruct these outliers, this paper adopts an anomaly detection model based on the Bidirectional Long Short-Term Memory Network (Bi-LSTM). Bi-LSTM consists of a forward LSTM and a backward LSTM network structure, capable of simultaneously extracting abstract features from historical data in both directions. Bi-LSTM inherits the long-term memory capability and forgetting mechanism of LSTM through its gated structure, and its bidirectional information flow significantly enhances its ability to capture the contextual information of vibration data. At each time step, Bi-LSTM updates the hidden states in

both directions, allowing for a more comprehensive extraction of features from time-series data. This characteristic enables Bi-LSTM to exhibit higher prediction accuracy and performance in long-term forecasting tasks, such as predicting wind-induced acceleration responses under temperature variation conditions, which are highly sensitive to historical and future data. Bi-LSTM provides an effective solution for reconstructing anomalies in bridge vibration acceleration time-series data under temperature variation conditions, enabling a more precise understanding and exploration of the dynamic changes and long-term dependencies within such data.

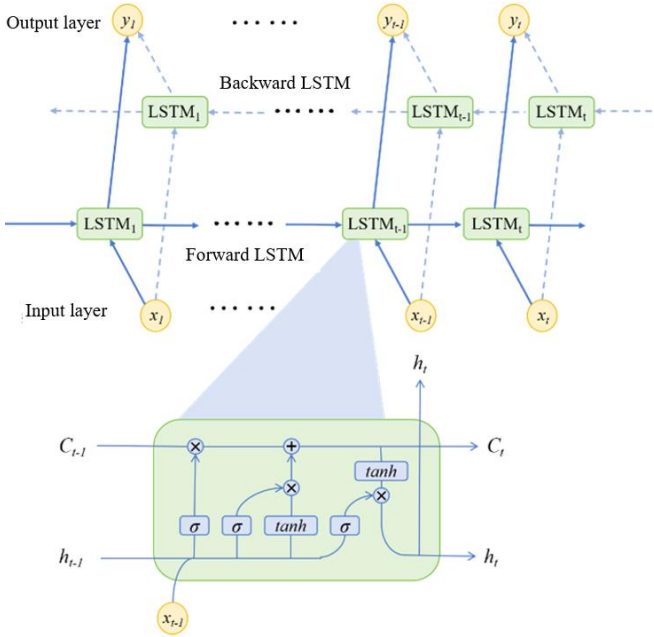

Figure 6. Bi-LSTM algorithm structure diagram

The Bi-LSTM algorithm uses LSTM units as its basic building blocks. The fundamental structure of an LSTM unit is shown in Figure 6. An LSTM unit consists of an input gate, forget gate, output gate, and cell state. These gates control the flow of information and memory updates, allowing the network to capture the long-term dependencies of bridge vibration sequences while preventing gradient vanishing or exploding problems when processing long sequences.

The forget gate (f_t) in LSTM is used to determine which information in the cell state c_{t-1} should be ignored. At the current time step t, the input data is x_t, and the output from the cell of the previous time step t-1 is h_{t-1}. The bias term for f_t is b_f, and the weight matrices are $W_{f,x}$ and $W_{f,h}$. After being processed by the sigmoid activation function σ, the output of the forget gate f_t is:

$$f_t = \sigma(W_{f,x}x_t + W_{f,h}h_{t-1} + b_f) \tag{16}$$

The sigmoid activation function is defined as:

$$\sigma(x) = \frac{1}{1+e^{-x}} \tag{17}$$

The LSTM layer determines the new information to retain in the cell state (c_t). The values of the input gate (i_t) and the new candidate value ($c\tilde{}_t$) at time step t are calculated as follows:

$$i_t = \sigma(W_{i,x}x_t + W_{i,h}h_{t-1} + b_i) \tag{18}$$

$$c_t = \tanh(W_{c,x}x_t + W_{c,h}h_{t-1} + b_c) \tag{19}$$

The results obtained from the previous steps are used to compute the new cell state c_t:

$$c_t = f_t \times c_{t-1} + i_t \times c_t \tag{20}$$

The output h_t of the LSTM layer's memory unit is as follows:

$$o_t = \sigma(W_{o,x}x_t + W_{o,h}h_{t-1} + b_o) \tag{21}$$

$$h_t = o_t \times \tanh(c_t) \tag{22}$$

The tanh activation function is defined as:

$$\tanh(x) = \frac{e^x - e^{-x}}{e^x + e^{-x}} \tag{23}$$

For Bi-LSTM, the architecture consists of forward and backward LSTM layers. The outputs of the forward and backward layers are processed simultaneously by the output layer as follows:

$$\overrightarrow{h_t} = \overrightarrow{LSTM}(W_1x_t + W_2\overrightarrow{h_{t-1}} + \vec{b}) \tag{24}$$

$$\overleftarrow{h_t} = \overleftarrow{LSTM}(W_3x_t + W_5\overleftarrow{h_{t-1}} + \vec{b}) \tag{25}$$

$$y_t = W_4\overrightarrow{h_t} + W_6\overleftarrow{h_t} + b_y \tag{26}$$

where, Eqs. (24) and (25) are the output vectors of the forward and backward LSTM, respectively, and W_1, W_2, W_3, W_4, W_5, W_6 are the corresponding weight vectors. y_t is the final output of Bi-LSTM at time step t.

4.3 Anomaly data reconstruction

The main idea of this study is to transform the problem of anomaly reconstruction for bridge vibration data under temperature variations into a problem of data prediction and judgment with learning behavior. First, the measured data under temperature variation conditions is preprocessed. Then, the Bi-LSTM model is utilized to model the temporal relationships between the bridge wind-induced vibration acceleration data under varying temperature conditions. Finally, the predicted acceleration data is obtained as the reconstructed anomaly data.

4.3.1 Data preprocessing

The measured bridge vibration data under temperature variation conditions is preprocessed. Assume the raw data is $X=\{x_1,x_2,\ldots x_{m-1},x_m\}$. First, non-numerical data is removed to obtain an m-dimensional array $X^*=\{x^*_1,x^*_2,\ldots x^*_{m-1},x^*_m\}$. Then, normalization is performed on X^* using Eq. (12):

$$\tilde{X}^* = \frac{X^* - \min(X^*)}{\max(X^*) - \min(X^*)} \tag{27}$$

The normalized data is then grouped, with the regression step size set to p. The input and output data sequences of the Bi-LSTM model are represented by Eqs. (28) and (29), respectively:

$$X_{in} = \{\tilde{x}_1^*, \tilde{x}_2^*, \cdots, \tilde{x}_{p-1}^*, \tilde{x}_2^*, \tilde{x}_3^*, \cdots, \tilde{x}_p^*, \cdots, \tilde{x}_l^*, \tilde{x}_{l+1}^*, \cdots, \tilde{x}_{l+p-2}^*, \cdots\} \quad (28)$$

$$X_{out} = \{\tilde{x}_p^*, \tilde{x}_{p+1}^*, \cdots, \tilde{x}_{p+l-1}^*, \cdots\} \quad (29)$$

4.3.2 Bi-LSTM network algorithm training

After preprocessing, the measured bridge vibration data under temperature variation conditions is fed into the Bi-LSTM model for training. During the forward propagation, forward calculations are performed from t=0 to t=n for the forward hidden layer weight matrix V_t and output h_t, and the forward weight matrix V_t is saved. Similarly, in the backward propagation, calculations are performed in reverse from t=n to t=0, obtaining the backward hidden layer weight matrix V'_t and output h'_t, with the reverse weight matrix V'_t saved. Finally, the total weight matrix V^* is obtained by summing the forward and backward weight matrices at corresponding time points. To train the predictive model, the Mean Squared Error (MSE) loss function is defined as follows:

$$MSE(y, \hat{y}) = \frac{1}{m}\sum_{i=1}^{m}(y_i - \hat{y}_i)^2 \quad (30)$$

where, y is the actual output data as a one-dimensional array, $\hat{y}$ is the predicted data as a one-dimensional array, and m is the length of the prediction data.

In this study, the Bi-LSTM model employs the Adam optimizer and completes the training of all grouped units through multiple iterations. The predicted values X_{pre} are calculated from the input data sequence X_{in}. Anomaly scores are obtained by comparing the predicted values X_{pre} and measured values X_{out} for anomaly detection.

4.4 Model architecture diagram

This study uses high-precision sensors installed at critical positions of the bridge structure to collect real-time vibration data under temperature variation conditions during construction. The data is transmitted wirelessly to storage devices. A dataset is then constructed, and anomaly detection is performed. This phase uses the Anomaly Transformer model to analyze the stored data. By employing a self-attention mechanism, the model learns the global and local correlations at each time point in the time series and calculates the correlation difference for each data point. The model effectively detects various types of anomalies, such as isolated outliers, continuous anomalies, and missing data, and marks these anomalies. Finally, the Bi-LSTM model is used to reconstruct the anomaly data. Since the bridge vibration acceleration data exhibits temporal dependency, the bidirectional network structure of Bi-LSTM fully leverages forward and backward information in the time series. By learning the temporal patterns of normal data, it generates reconstructed data consistent with the vibration characteristics of the bridge. The model architecture is illustrated in Figure 7.

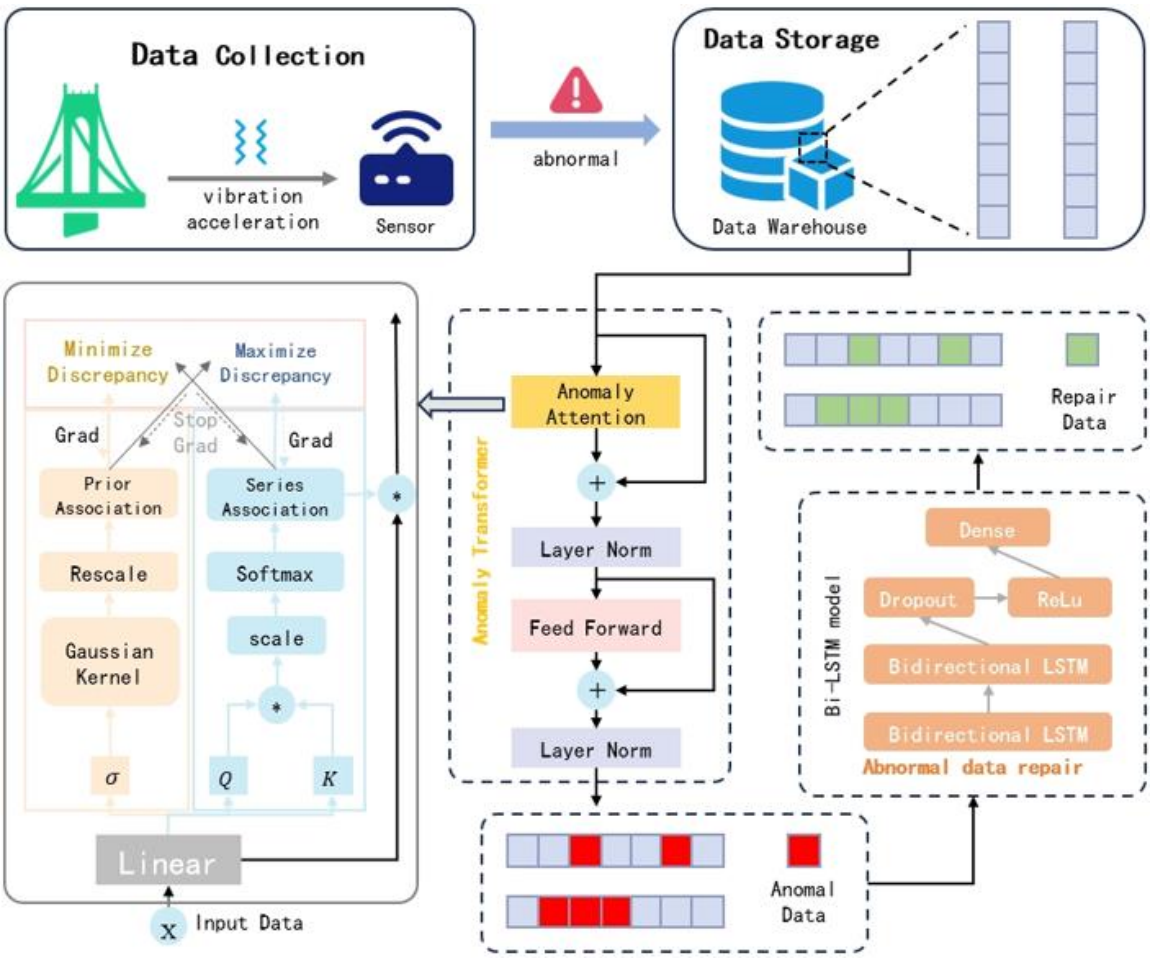

Figure 7. Model architecture diagram

5. EXPERIMENTS AND RESULTS ANALYSIS

5.1 Description of experimental dataset

The data used in this study are obtained from the main bridge of the Toutunhe Interchange Connection Line in Urumqi, Xinjiang, which is currently under construction. By deploying acceleration sensors on the bridge, the vibration acceleration of the bridge is collected. Due to various activities during the construction process, such as equipment operation, material transportation, and changes in the construction environment, the data contain rich dynamic response characteristics and anomalies. These data provide an essential foundation for studying the structural behavior of bridges under complex working conditions, and they serve as an ideal experimental dataset for verifying the anomaly data detection and reconstruction models. The measured bridge vibration acceleration data collected are used to construct the dataset, totaling 41,600 records, with 30,000 records as the training set and 11,600 records as the testing set. Detailed information is shown in Table 1.

Table 1. Details of the dataset

Category	Training Set	Testing Set
Data Volume	30000	11600
Maximum Value (/m·s²)	9.53×10^{-3}	12.2×10^{-4}
Minimum Value (/m·s²)	-8.18×10^{-3}	-6.81×10^{-4}
Mean Value (/m·s²)	1.53×10^{-4}	1.69×10^{-4}
Variance (/m·s²)	1.8×10^{-6}	1.57×10^{-6}
Number of Anomalies	-	1732

5.2 Evaluation metrics

To evaluate the performance of the model, this paper uses the following evaluation metrics: Accuracy, Precision, Recall, and $F1$-score. According to the anomaly judgment rules, the actual values and predicted values are compared and divided into four categories. The details can be seen in the confusion matrix shown in Table 2.

Table 2. Confusion matrix

Classification of Results	Predicted Anomalies	Predicted Normal Values
Actual Anomalies	*TP*	*FN*
Actual Normal Values	*FP*	*TN*

TP (True Positive): The number of anomalies correctly identified.

TN (True Negative): The number of normal data correctly identified.

FP (False Positive): The number of normal data misclassified as anomalies.

FN (False Negative): The number of anomalies misclassified as normal data.

Accuracy is defined as the ratio of correctly predicted samples to the total number of samples:

$$Accuracy = \frac{TP + TN}{TP + FP + TN + FN} \tag{31}$$

Precision is defined as the ratio of correctly predicted anomaly samples to all samples predicted as anomalies:

$$Precision = \frac{TP}{TP + FP} \tag{32}$$

Recall is defined as the ratio of correctly predicted anomaly samples to the actual anomaly samples:

$$Recall = \frac{TP}{TP + FN} \tag{33}$$

$F1$-score is defined as the harmonic mean of Precision and Recall:

$$F1\text{-}score = 2 \times \frac{Precision \times Recall}{Precision + Recall} \tag{34}$$

In the anomaly detection problem, it is crucial to detect as many anomalies as possible rather than misclassify normal values as anomalies. The $F1$-score is an evaluation metric that considers both Precision and Recall, and a higher $F1$-score indicates better classifier performance.

5.3 Analysis of bridge vibration characteristics under different temperature changes

From the data presented in Table 3 and Figure 8, it is evident that as the temperature difference increases, the maximum frequencies of the bridge change significantly. For instance, when ΔT = 455℃, the 1st order frequency of the bridge is 15.236 Hz, and the 2nd order frequency is 15.369 Hz. When the temperature difference increases to 562℃, the 1st order frequency decreases to 1.562 Hz, and the 2nd order frequency decreases to 1.548 Hz. This indicates that the frequencies decrease as the temperature load increases. Simultaneously, the lower limit of the maximum cross-section area of the bridge gradually increases with the temperature load. For example, when ΔT = 455℃, the minimum cross-section area is 0.0256, which increases to 0.0554 at ΔT = 562℃. This suggests that as the temperature load increases, the bridge's materials need to concentrate more in the central section to ensure structural stability. This phenomenon may result from changes in the force distribution under high-temperature conditions. To maintain stiffness and load-bearing capacity, bridge design emphasizes resistance to bending, stretching, and other deformations under temperature loads.

Table 3. Maximum vibration frequencies of the bridge under high-temperature load

Δ*T*	455	512	562
Maximum cross-sectional area lower limit	0.0256	0.0345	0.0554
1st Order Frequency (Hz)	15.236	11.235	1.562
2nd Order Frequency (Hz)	15.369	11.257	1.548

Figure 8 illustrates the cross-section distribution of maximum frequencies under different temperature differences. It shows that with greater temperature loads, the materials of the bridge concentrate more in the middle section. This is likely because, under larger temperature differences, the central region of the bridge is more susceptible to stress changes caused by thermal expansion. Increasing material

concentration in this area enhances stiffness and resistance to thermal deformation. This optimization design reduces vibration frequency fluctuations due to temperature changes, improving the accuracy of anomaly detection in vibration acceleration.

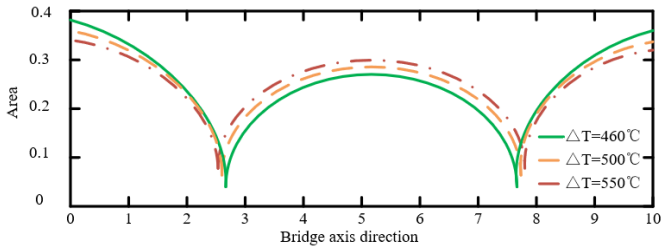

Figure 8. Cross-section distribution of maximum vibration frequencies under high-temperature load

Table 4. Maximum vibration frequencies of the bridge under low-temperature load

ΔT	0	101	214
Maximum cross-sectional area lower limit	0.0001	0.0042	0.132
1st Order Frequency (Hz)	72.325	52.326	37.225
2nd Order Frequency (Hz)	72.315	52.124	38.659

Table 4 lists the vibration frequencies and the minimum cross-section area of the bridge under different low-temperature differences (ΔT). As the temperature difference increases, the vibration frequencies of the bridge decrease. For instance, when ΔT = 0℃, the 1st order frequency is 72.325 Hz, and the 2nd order frequency is 72.315 Hz. When the temperature difference increases to 214℃, the 1st order frequency decreases to 37.225 Hz, and the 2nd order frequency decreases to 38.659 Hz. This trend indicates that increasing low-temperature loads gradually reduces the vibration frequencies of the bridge. This change can be attributed to the effect of low temperatures on bridge materials. Low temperatures may make materials brittle, altering stiffness and elastic modulus, which affects the dynamic characteristics of the structure. Additionally, as the temperature difference increases, the minimum cross-section area of the bridge gradually increases. Specifically, when ΔT = 0℃, the minimum cross-section area is 0.0001, which increases to 0.1321 at ΔT = 214℃. This suggests that to maintain the safety and stability of the bridge structure, the design requires more materials to concentrate at the ends of the beam under increasing low-temperature loads.

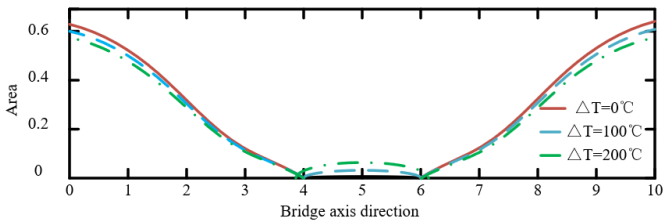

Figure 9. Cross-section distribution of maximum vibration frequencies under low-temperature load

Figure 9 shows the cross-section distribution of maximum frequencies under different initial temperature differences. Under low-temperature loads, the bridge materials primarily concentrate at the beam ends. This is likely due to concentrated forces at the ends of the bridge in low-temperature environments. As the temperature difference increases, material distribution in the middle section of the beam gradually increases, while material concentration at the ends decreases. This indicates that as the temperature further decreases, the middle section of the bridge requires more materials to maintain structural balance and stiffness, while the ends may see reduced material concentration due to increased brittleness at low temperatures.

Table 5. Maximum vibration frequencies of the bridge under medium thermal load

ΔT	312	401
1st Order Frequency (Hz)	25.265	22.325
2nd Order Frequency (Hz)	42.236	22.154
Maximum cross-sectional area lower limit	0.0326	0.0236

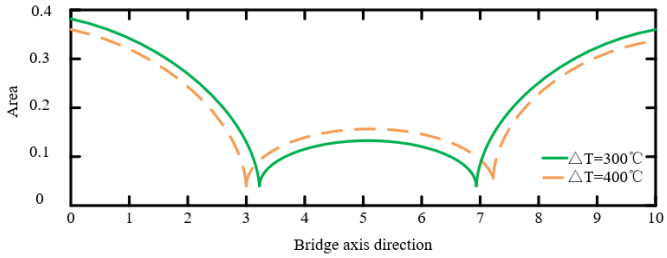

Figure 10. Cross-sectional area distribution diagram of the bridge's maximized vibration frequency under medium thermal load

According to the data in Table 5, under medium thermal load (ΔT from 312℃ to 401℃), the optimal design solution for maximizing the bridge's vibration frequency is a single-mode solution. Even when the maximum cross-sectional area lower limit is reduced, or approaches zero, the system still chooses the single-mode optimal solution rather than the multi-mode solution. This is different from the situation under low and high-temperature conditions. At low and high temperatures, due to the changes in the material and structural properties of the bridge, a heavy-mode optimal solution is more likely to appear. Figure 10 shows the distribution of the cross-sectional area for the maximum vibration frequency of the bridge under the application of medium-temperature loads. The experimental results show that under medium thermal load, the temperature variation has a relatively small effect on the stiffness of the bridge, so there is no significant multi-mode vibration trend in the bridge system. At this point, the beam's structure tends to choose a simplified single-mode design to achieve frequency maximization. In other words, under medium temperature differences, the temperature variation is insufficient to induce multi-modal vibration responses in the bridge structure. When the temperature difference is within a medium range, the force differences at both ends and the middle of the bridge are relatively small, and the structure no longer needs to rely on multi-mode vibration to adapt to the non-uniform stress distribution caused by temperature differences. Therefore, the system will choose a more simplified single-mode structure, minimizing design complexity while still achieving the goal of maximizing vibration frequency.

In combination with the research objectives of this paper, especially when constructing the vibration acceleration anomaly detection model for bridges under temperature variation conditions, the impact of different temperature

ranges on the vibration modes of the bridge must be considered:

(1) In low and high-temperature environments, the bridge's vibration frequency and acceleration variations are usually more significant and may involve complex multi-mode responses. Therefore, the anomaly detection model for vibration acceleration should pay more attention to the multi-modal characteristics of the frequency.

(2) In an environment with medium temperature differences, the bridge's vibration frequency optimization tends toward a single mode, and the model should be simplified to focus on identifying small changes or anomalies caused by temperature through single-mode analysis.

Therefore, for different temperature load ranges, a corresponding vibration acceleration anomaly detection model should be designed. For bridges under medium thermal load, single-mode vibration analysis may be more effective; while at extreme temperatures, more multi-mode features should be considered to improve the sensitivity and accuracy of detection.

5.4 Bridge vibration acceleration anomaly data detection

Due to the influence of the operating environment and equipment status of the bridge structural health monitoring system, data anomalies may occur during the data collection process, leading to inaccurate bridge structural health assessments in the later stages, which may seriously affect bridge operation. Therefore, accurate anomaly data detection is crucial. In this paper, the Anomaly Transformer algorithm is used to detect anomaly data in the bridge structural health monitoring acceleration data, with the main anomaly types being isolated anomalies and continuous anomalies.

5.4.1 Isolated anomaly detection

Isolated anomalies, as shown in Figure 11, usually manifest as single data points deviating from normal values. This type of anomaly is often caused by the complex operating environment of data collection equipment, where the sensors are affected by environmental factors, leading to inaccurate measurements and, thus, data anomalies. In this scenario, the Anomaly Transformer can capture the local and global correlations of each time point in the time series through the self-attention mechanism. When the correlation of a data point is significantly lower than that of normal data points, the model can effectively identify the point as an isolated anomaly.

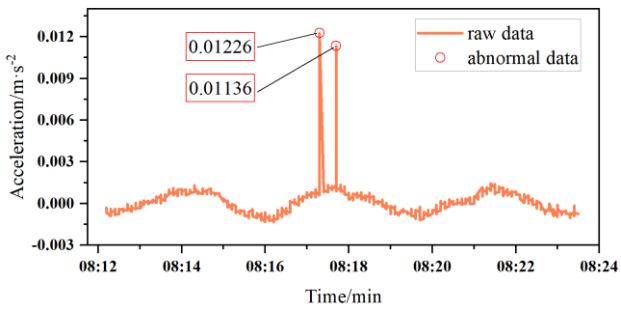

Figure 11. Isolated anomaly detection result chart

5.4.2 Continuous anomaly detection

Continuous anomalies mainly include two types: continuous missing value anomalies and continuous data pattern anomalies, as shown in Figure 12. These include anomalies caused by data loss or damage during transmission from the data collection device to the storage system, possibly due to network failures, signal interference, etc., leading to missing data anomalies. Furthermore, during the data collection, if the bridge is in a construction state, ground disturbances, frequent movement of mechanical equipment, and transportation of materials can cause the bridge structure to experience abnormal stress and deformation in a short time. This interference is more obvious, especially when the construction equipment is close to the bridge or directly affects the bridge structure, and it can significantly affect the accuracy of monitoring data. In continuous anomaly scenarios, the Anomaly Transformer can identify these continuous anomaly regions through sequence correlations. Especially for continuous missing values, the model can detect abnormal areas by the significantly low correlation of adjacent time points.

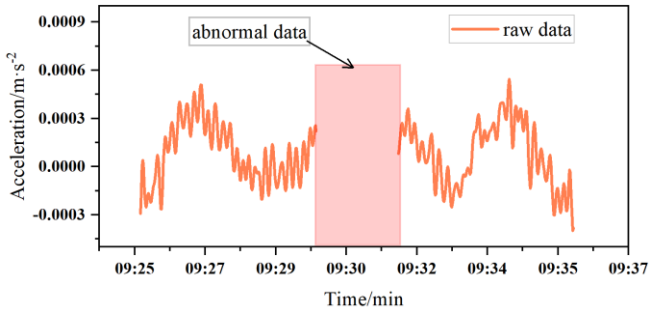

(a) Continuous missing value anomaly

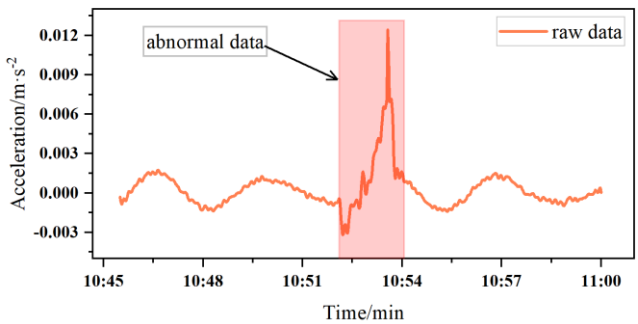

(b) Continuous data pattern anomaly

Figure 12. Continuous anomaly detection results

Figure 13 shows the confusion matrix for the four models on the test set. In the bridge acceleration data anomaly detection problem, the motion characteristics of abnormal points differ significantly from those of adjacent normal points. From the results in Figure 14 and Table 6, it can be seen that the RNN model has slightly lower precision and $F1$-score compared to other models. Although the RNN model can capture the dependencies between time points when handling time series data, its recurrent structure makes it prone to gradient vanishing or explosion problems when processing long sequence data. This limits the model's ability to capture long-term dependencies, especially in the complex bridge acceleration data, where its performance does not meet expectations. In addition, the LSTM model has slightly higher precision than the GRU model, indicating an advantage in capturing subtle features in the data. However, its recall and $F1$-score are slightly lower, which may be related to the memory unit design of the LSTM. In some cases, LSTM may face challenges in memory retention, especially when dealing with sparse anomalous points, limiting the model's ability to detect anomalies.

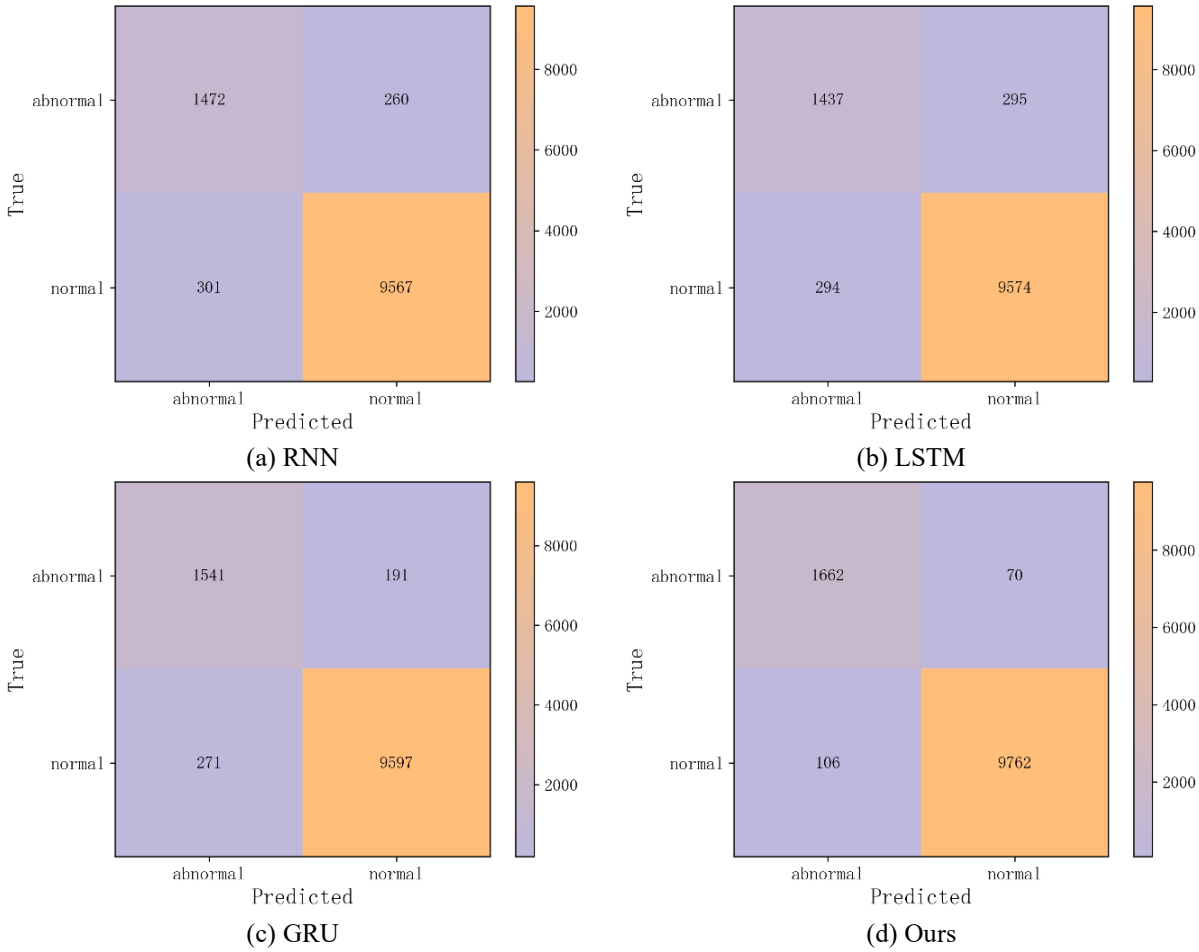

Figure 13. Confusion matrix for four models on the test set

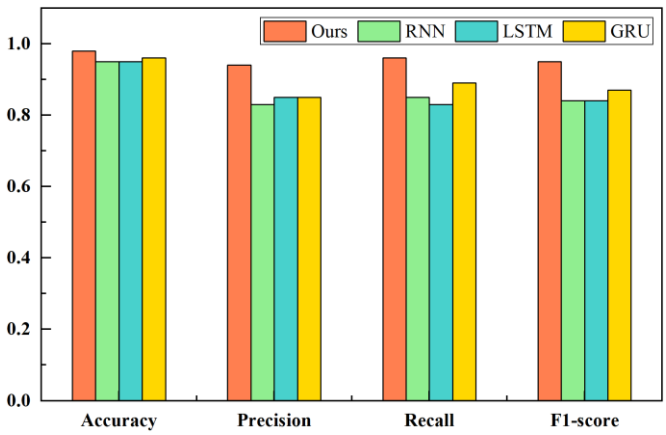

Figure 14. Comparison of evaluation metrics for different models

Table 6. Performance metrics for different models

Predictive Models	Accuracy	Precision	Recall	*F*1-Score
RNN	0.95	0.83	0.85	0.84
LSTM	0.95	0.85	0.83	0.84
GRU	0.96	0.85	0.89	0.87
Ours	0.98	0.94	0.96	0.95

GRU performs well in both short-term and long-term dependencies, and in the experiments, its recall rate is higher than LSTM's. This indicates that GRU has an advantage in detecting anomalies, especially when the anomalies are sparse and the dynamic features are complex. While GRU's overall performance is similar to LSTM, its simpler structure allows it to have better computational efficiency in practical applications. The Anomaly Transformer model outperforms in accuracy, precision, recall, and *F*1-score. Its unique bidirectional network unit structure quickly adjusts the relationship between current and past/future data, effectively associating contextual information. The Anomaly Transformer model can effectively mine the motion characteristics of time series data, avoiding complex function relationship estimation, improving prediction accuracy, and providing strong support for subsequent anomaly detection and judgment problems.

5.5 BiLSTM bridge vibration acceleration anomaly data reconstruction

In the anomaly detection task, we have successfully identified and located anomalous points using the Anomaly Transformer model. Next, in order to ensure the validity and availability of the bridge health monitoring system data, we need to reconstruct the anomalous data. Through effective reconstruction methods, we can restore the integrity and continuity of the data, thus improving the reliability of the bridge structural health assessment results.

Since bridge vibration acceleration data has strong correlation and dependence on the time dimension, the current acceleration value is influenced by both past and future acceleration values. It also has complex dynamic patterns, such as periodic and trend changes. Therefore, for the anomaly

data reconstruction, we use the BiLSTM model, which can simultaneously capture the contextual information in both directions when processing time series data. By processing the data in both forward and backward LSTM networks, BiLSTM can better understand the dynamic characteristics of time series, thereby improving its ability to reconstruct anomalous data. During the reconstruction process, BiLSTM uses its bidirectional structure, combining information from the current moment and its previous and subsequent moments, to precisely reconstruct the anomalous data. This not only restores the original trends and patterns of the data but also provides more accurate results in the repair of anomalous data.

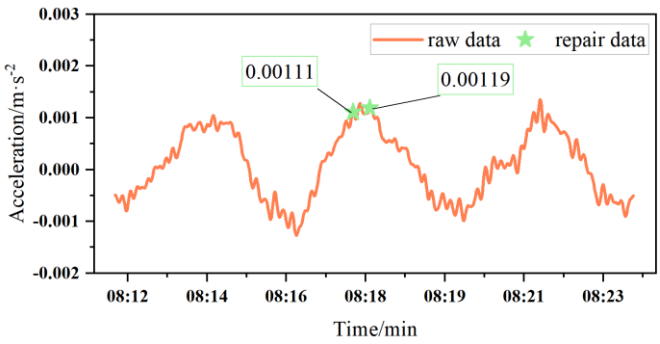

(a) Anomaly reconstruction of data points

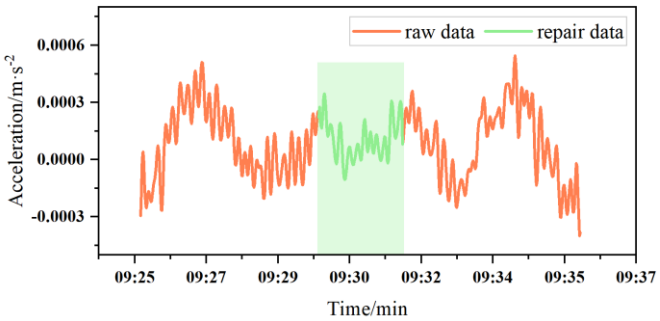

(b) Anomaly reconstruction of missing data

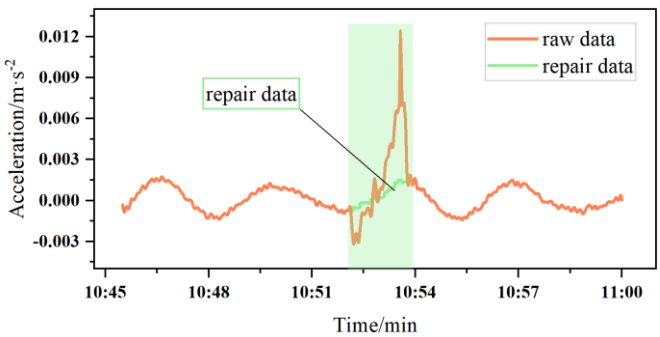

(c) Anomaly reconstruction of data patterns

Figure 15. Anomaly data reconstruction

There are three main types of anomalies in bridge vibration acceleration data: isolated data anomalies, continuous missing value anomalies, and continuous data pattern anomalies. For these three types of anomalous data, this paper uses the BiLSTM model to reconstruct the bridge vibration acceleration anomaly data. The reconstruction results of anomalous data are shown in Figure 15. The experimental results show that the BiLSTM model performs well in anomaly data reconstruction. It can effectively restore the original trends and periodic features of the anomalous data, significantly reducing the difference between the reconstructed data and the actual observed data. This result indicates that BiLSTM can provide accurate and reliable reconstruction when handling bridge vibration acceleration data with significant time dependencies and complex dynamic patterns, significantly enhancing the integrity and reliability of the data.

6. CONCLUSION

This paper aims to address the limitations in current bridge health monitoring systems concerning vibration acceleration anomaly detection under temperature variation conditions. By analyzing the impact of temperature changes on the bridge's vibration characteristics, this study revealed the specific mechanisms through which temperature affects vibration frequency and mode, finding that temperature changes significantly alter the bridge's vibration response. Based on this, the paper constructed a bridge vibration acceleration dataset that includes temperature factors and combines temperature data for feature extraction and analysis, proposing an anomaly detection model that adapts to temperature changes. The experimental results show that the proposed model can effectively handle the effects of temperature variations, improving the accuracy and robustness of anomaly detection.

Overall, this research has important theoretical value and practical significance. First, the proposed model fills the gap in existing studies that have not adequately considered temperature variations, providing a new technological approach. Second, the constructed dataset provides data support for future research and offers a new method for bridge health monitoring. However, there are some limitations in this study, such as experimental environment constraints and a limited dataset size. Future work could further optimize the model through field data validation and research on multiple types of bridges. Future research directions may focus on field data collection and model validation, the application of deep learning technologies, and exploration of multi-sensor fusion technologies. Additionally, by combining IoT and cloud computing technologies, an intelligent bridge health monitoring system could be developed for more accurate real-time monitoring and remote diagnostics. In conclusion, this paper provides strong theoretical support and technical guidance for bridge health monitoring under temperature variation conditions, and future research can further enhance the adaptability and practicality of the model.

REFERENCES

[1] Yin, Z.H., Li, Y.F., Yang, Z.H. (2012). Temperature prediction for massive concrete in bridge structure based on PSO and RVM. Information, 15(10): 4321-4328.

[2] Chinh, L. M. (2021). Proposed SHM system with acoustic emission (AE) technology for Tran Hoang Na steel arch bridge. International Journal of GEOMATE, 21(84): 210-219. https://doi.org/10.21660/2021.84.j2190

[3] Wang, S., Zhang, G., Li, J., Wang, Y., Chen, B. (2023). Temperature response of double-layer steel truss bridge girders. Buildings, 13(11): 2889. https://doi.org/10.3390/buildings13112889

[4] Chen, Y., Wang, Y., Song, A., Zhao, L. (2024). Effects

of high-temperature environments on the thermodynamic performance of reinforced concrete bridge structures. International Journal of Heat and Technology, 42(5): 1541-1550. https://doi.org/10.18280/ijht.420507

[5] Fu, M., Liang, Y., Wu, B., Zhang, L., Tang, G. (2022). Research on deformation analysis and rehabilitation for a beam-arch combination bridge suffering an extreme temperature field. Applied Sciences, 12(14): 6909. https://doi.org/10.3390/app12146909

[6] Song, Z. (2023). Enhancing bridge structural stability: A comprehensive analysis of thermodynamic properties and thermal stress performance. International Journal of Heat and Technology, 41(3): 761-768. https://doi.org/10.18280/ijht.410333

[7] Xue, G., Miao, J., Zhang, D., Zuo, S., Zhang, C., Li, N. (2025). Seismic acceleration response prediction method of the PSCFST bridge based on TCN. Journal of Constructional Steel Research, 224: 109147. https://doi.org/10.1016/j.jcsr.2024.109147

[8] Sun, Y.Y., Xu, Z.Y., Wang, Z.H. (2024). Assessment of fatigue life in H-type bridge hangers subjected to torsional vibration. Journal of Civil and Hydraulic Engineering, 2(3): 131-141. https://doi.org/10.56578/jche020301

[9] Niu, Q.C., Guo, X.H. (2023). Application of a thermodynamic model in durability analysis of bridge structures under climatic variability. International Journal of Heat and Technology, 41(4): 901-909. https://doi.org/10.18280/ijht.410412

[10] Naser, A.F., Mohammed, H.A., Mohammed, A.A. (2021). Mathematical modeling of linear static and dynamic analysis for pier height effect on the structural performance of bridges structures. Mathematical Modelling of Engineering Problems, 8(4): 617-625. https://doi.org/10.18280/mmep.080415

[11] Chen, Y., Zhang, G.Q., Song, A., You, P.B. (2024). Thermodynamic properties of composite material bridges under thermal cycling. International Journal of Heat and Technology, 42(1): 171-182. https://doi.org/10.18280/ijht.420118

[12] Lee, J.L., Tyan, Y.Y., Wen, M.H., Wu, Y.W. (2018). Applying ZigBee wireless sensor and control network for bridge safety monitoring. Advances in Mechanical Engineering, 10(7): 1687814018787398. https://doi.org/10.1177/1687814018787398

[13] Su, H., Guo, C., Han, T., Li, R., Liu, Z., Su, F., Shang, L. (2023). Research on safety state evaluation of cable-stayed bridge structures across the sea. Journal of Marine Science and Engineering, 11(11): 2034. https://doi.org/10.3390/jmse11112034

[14] Zhou, J., Yang, J. (2011). Analysis of bridge safety assessment with correlation between measuring points for bridge health monitoring. Intelligent Automation & Soft Computing, 17(5): 643-650. https://doi.org/10.1080/10798587.2011.10644199

[15] Yu, J., Li, C., Sun, Q. (2020). Field loading-test based SHM system safety standard determination. Stavební obzor-Civil Engineering Journal, 29(2): 229-244. https://doi.org/10.14311/CEJ.2020.01.0020

[16] Zhu, E., Bai, Z., Zhu, L., Li, Y. (2022). Research on bridge structure SAM based on real-time monitoring. Journal of Civil Structural Health Monitoring, 12(3): 725-742. https://doi.org/10.1007/s13349-022-00571-7

[17] Huang, F.L., He, X.H., Chen, Z.Q., Zeng, C.H. (2004). Structural safety monitoring for Nanjing Yangtze river bridge. Journal of Central South University of Technology, 11: 332-335. https://doi.org/10.1007/s11771-004-0068-4

[18] Wang, L.B., Jiang, P.W. (2016). Research on the computational method of vibration impact coefficient for the long-span bridge and its application in engineering. Journal of Vibroengineering, 18(1): 394-407.

[19] Cheng, M.Y., Liao, K.W., Chiu, Y.F., Wu, Y.W., Yeh, S.H., Lin, T.C. (2022). Automated mobile vibration measurement and signal analysis for bridge scour prevention and warning. Automation in Construction, 134: 104063. https://doi.org/10.1016/j.autcon.2021.104063

[20] Le, H.X., Hwang, E.S. (2017). Investigation of deflection and vibration criteria for road bridges. KSCE Journal of Civil Engineering, 21: 829-837. https://doi.org/10.1007/s12205-016-0532-3

[21] Zhou, L., Ge, Y. (2008). Wind tunnel test for vortex-induced vibration of vehicle-bridge system section model. Journal of the Brazilian Society of Mechanical Sciences and Engineering, 30: 110-117. https://doi.org/10.1590/S1678-58782008000200003

[22] Wang, H., Qin, S. (2016). Taigu pedestrian bridge in China. Structural Engineering International, 26(1): 74-78. https://doi.org/10.2749/101686615X14355644770893

[23] Fujino, Y., Siringoringo, D. (2013). Vibration mechanisms and controls of long-span bridges: A review. Structural Engineering International, 23(3): 248-268. https://doi.org/10.2749/101686613X13439149156886

[24] Liu, Y., Yan, W., Yin, X., Wang, L., Han, Y. (2022). Vibration analysis of the continuous beam bridge considering the action of jump impacting. Advances in Structural Engineering, 25(13): 2627-2640. https://doi.org/10.1177/13694332221105706